Triple Helix Formation with *Drosophila* Satellite Repeats. Unexpected Stabilization by Copper Ions[†,‡]

Virginie Horn,[§,||] Laurent Lacroix,[⊥] Thierry Gautier,[§] Masashi Takasugi,[⊥] Jean-Louis Mergny,[⊥] and Jérôme Lacoste*[,#]

Laboratoire de Biologie Moléculaire et Cellulaire de la Différenciation, INSERM UR 309, Institut Albert Bonniot, Rond-point de la Chantourne, 38700 Grenoble, France, Laboratoire de Biophysique, Muséum National d'Histoire Naturelle, USM 0503, INSERM UR 565, CNRS UMR 5153, 43 rue Cuvier, 75231 Paris Cedex 05, France, Laboratoire d'Etudes de la Différenciation et de l'Adhérence Cellulaire, CNRS UMR 5538, Institut Albert Bonniot, Rond-point de la Chantourne, 38700 Grenoble, France, and Laboratoire des Radiopharmaceutiques Biocliniques, INSERM 0340, Faculté de Médecine de Grenoble, 38700 La Tronche, France

Received April 9, 2004; Revised Manuscript Received June 21, 2004

ABSTRACT: The *Drosophila melanogaster* $(AAGAGAG)_n$ satellite repeat represents up to 1.5% of the entire fly genome and may adopt non-B DNA structures such as pyrimidine triple helices. UV melting and electrophoretic mobility shift assay experiments were used to monitor the stability of intermolecular triple helices as a function of size, pH, and backbone or base modification. Three to four repeats of the heptanucleotide motif were sufficient to allow the formation of a stable complex, especially when modified TFOs were used. Unexpectedly, low concentrations (40−100 μM) of Cu^{2+} were found to favor strongly pyrimidine triplex formation under near-physiological conditions. In contrast, a much higher magnesium concentration was required to stabilize these triplexes significantly, suggesting that copper may be an essential stabilizing factor for pyrimidine triplexes.

A notable feature of higher eukaryotic genomes is that certain portions show remarkably different properties from the bulk of the DNA. These were first distinguished from euchromatin cytologically, on the basis of differential staining properties, and named heterochromatin by Heitz (*1*). Molecular and genetic properties that further distinguish heterochromatin from euchromatin include DNA sequence composition, replication timing, condensation throughout the cell cycle, and the ability to silence gene expression (see refs *2*−*4* for a review). Heterochromatin is especially abundant at the centromeres and telomeres and is composed of highly reiterated sequences characterized by their unusual base composition and nature and called satellite DNAs. For example, in *Drosophila melanogaster*, heterochromatin accounts for an estimated 33.5% of the female genome with satellite repeats representing 21% of the genome (*4*, *5*). Progress has been made in the understanding of the sequence and molecular organization of *Drosophila* (*5*−*7*) and human (*8*) centromeres, yet our understanding of their higher structural organization and function is still very limited.

Centromere function may be achieved by formation of a specific higher order structure (*7*, *9*−*11*), an overall three-dimensional organization that results from special DNA architectures (bending, triplex or quadruplex DNA) and/or DNA−protein interaction in the centromere [GAGA factor (GAF) in *Drosophila* (*12*), Ikaros in mice (*13*), HP1 in human (*14*)]. For example, the AG-rich satellite DNAs found in the four *D. melanogaster* centromeres may be examples of sequences that could participate in or even promote a centromere-specific structure by adopting non-B DNA conformations. As a matter of fact, $(AAGAG)_n$ and $(AAGAGAG)_n$ *Drosophila* centromeric satellites (*4*) are polypurine−polypyrimidine tracts that can potentially adopt non-B DNA structures such as triple-stranded H-DNA or *H-DNA (*15*). Consistent with this hypothesis is the fact that the GAGA factor (GAF), a sequence-specific DNA-binding protein which specifically recognizes the $(AAGAG)_n$ and $(AAGAGAG)_n$ satellites (*12*, *16*), may also bind to triple-stranded DNA (*17*) or promote a link between two separate DNA molecules (*18*).

A DNA triplex is formed upon binding of a pyrimidine or a purine single-stranded DNA to the major groove of a double helix, forming Hoogsteen or reverse-Hoogsteen hydrogen bonds with the purine strand of the duplex. Triplex DNA comes in three structural classes that differ in the base composition of the third strand, the relative orientation of the phosphate−deoxyribose backbones, the sensitivity to pH and cations (*19*, *20*), and thermodynamic parameters (*21*). They have been described as the (C,T) or pyrimidine motif, the (G,A) or purine motif, and the (G,T) motif. These motifs can form both intramolecularly, giving H-DNA, and inter-

[†] This work was supported by ARC Grants 4321 and 3365 to J.-L.M.

[‡] This paper is dedicated to the memory of Professor Claude Hélène (1938−2003).

* Corresponding author. E-mail: jerl@ccr.jussieu.fr. Fax: (33-1) (0)4 76 63 71 42. Phone: (33-1) (0)4 76 63 71 33.

[§] Laboratoire de Biologie Moléculaire et Cellulaire de la Différenciation.

[||] Current address: Laboratoire d'Etudes de la Différenciation et de l'Adhérence Cellulaire, CNRS UMR 5538, Institut Albert Bonniot, Rond-point de la Chantourne, 38700 Grenoble, France.

[⊥] Muséum National d'Histoire Naturelle.

[#] Laboratoire des Radiopharmaceutiques Biocliniques.

10.1021/bi049287t CCC: $27.50
Published on Web 08/11/2004

molecularly with triple helix-forming oligonucleotides (TFOs).[1] In the pyrimidine motif, the third strand is composed of cytosines and thymines and binds parallel to the purine strand of the duplex by Hoogsteen hydrogen bonds, leading to the formation of T·A*T and C·G*C$^+$ triplets (*22*, *23*). Formation of this motif requires slightly acidic conditions (*22*, *23*). In the purine motif, the third strand is composed of guanines and adenines and binds antiparallel to the purine strand of the duplex by reverse-Hoogsteen hydrogen bonds, leading to the formation of T·A*A and C·G*G triplets (*22*−*24*). This motif contains no protonated bases, and its stability is therefore pH-independent. In the case of oligonucleotides, it generally requires divalent (Mg^{2+}, Zn^{2+}, Mn^{2+}, ...) (*19*) or multivalent cations (spermine, spermidine) (*22*) for its formation. It has also been shown that unimolecular folded purine triplexes can exist without any divalent cation and that the poly(dT)·2poly(dA) triplex can exist in the absence of divalent cation if high concentrations of monovalent cations are present (>1 M) (*25*, *26*). In the (G,T) motif the third strand is composed of guanines and thymines and binds parallel or antiparallel to the purine strand of the duplex (*27*, *28*).

Two main problems arise concerning the possibility of forming and stabilizing DNA triplexes in vivo. As noted above, the pyrimidine motif requires a slightly acidic pH, while the purine motif requires millimolar or higher concentrations of divalent cations (*15*). As a consequence, most studies have been oriented toward the formation and stabilization of DNA triplexes under near-physiological conditions, using base- or backbone-modified TFOs [i.e., 5-methyl-dC (*29*), 5-propynyl-dU (*30*), and 2′-*O*-methyl (*31*)].

In this report we address for the first time the possibility of forming triple helical structures with the *D. melanogaster* satellite sequence $(AAGAGAG)_{1-4}$ in vitro. We limited our analysis to the formation of intermolecular pyrimidine triplexes. UV melting experiments were used to monitor the stability of the triple helix as a function of size, pH, and backbone or base modification. EMSA experiments were used to confirm triplex formation, to determine their apparent dissociation constants (K_D), and to study the effect of divalent cations such as Mg^{2+} and Cu^{2+}. Several articles deal with the formation of triple helices with 5-methylcytosine and 2′-*O*-methyl TFOs (*31*−*33*), but few report this formation with morpholino TFOs (*34*, *35*), and to our knowledge, none study the effect of Cu^{2+}. We demonstrate that low concentrations (40−100 μM) of Cu^{2+} favor pyrimidine triplex formation under near-physiological conditions.

EXPERIMENTAL PROCEDURES

Oligonucleotides and Chemicals. Most oligonucleotides were synthesized by Eurogentec (Seraing, Belgium). Morpholino oligonucleotides (21TCmo) were synthesized by GeneTools, LLC (Philomath, OR). Concentrations of all oligonucleotides were estimated by UV absorption in water at 20 °C, using a nearest-neighbor approximation for the absorption coefficients of the unfolded species (*36*). All concentrations were expressed in strand molarity.

Nomenclature. Oligonucleotides used in this study are listed in Table 1. We adopted the following convention for all of the oligonucleotides: the first number refers to the length of the oligonucleotide followed by the strand composition (R, purine-rich strand of the duplex; Y, pyrimidine-rich strand of the duplex; TC, pyrimidine TFO), followed by the modification (e.g., OMe for 2′-*O*-methyl sugar, mC for methyl-substituted cytosine). Duplexes are referred to as 19 RY, 26 RY, 33 RY, and 40 RY; they contain 1, 2, 3, or 4 copies of the heptanucleotide motif, respectively. Concerning the base triplets, as an example, a T·A*T triplet is obtained when base T in the third strand recognizes the Watson−Crick T·A base pair and forms specific hydrogen bonds, "*", with the adenine of the duplex.

UV Absorption Spectrophotometry. Absorbance versus temperature heating and cooling curves were obtained using a KONTRON-UVIKON 940 spectrophotometer as previously described (*37*). The temperature of the bath was increased or decreased at a rate of 0.2 °C/min, thus allowing complete thermal equilibrium of the cuvettes. At each temperature, absorbance measurements were done at 245, 260, 295, and 405 nm (control wavelength). Most data were extracted from the profiles recorded at 245 nm, as the amplitude of the triplex transition was the largest at this wavelength (*34*). Unless otherwise specified, all experiments were performed in 10 mM sodium cacodylate buffer (pH 6.0 or 7.2) containing 100 mM KCl and various concentrations of $MgCl_2$ (0−10 mM). For triplex experiments strand concentrations ranged from 1.5 to 2.5 μM for the duplexes and from 1.8 to3 μM for the third strand. Self-association of a TFO alone was checked in the same concentration range as for triplex analysis. At near-neutral pH, the thermal dissociation (heating) curves of most triplexes were shifted toward higher temperatures as compared to the association (cooling) curves (see Figure 1B−D for an example). Such behavior, which is the result of slow association and dissociation kinetics, has already been described for triple helix formation. These profiles were not fully consistent with a simple two-state model, therefore excluding a quantitative analysis of the kinetic parameters of triplex formation as previously described (*38*). We therefore restricted our analysis to the simple determination of the temperature of half-dissociation "$T_{1/2}$" (upon heating), which slightly overestimates the true melting temperature (T_m). When profiles were consistent with a two-state model (TFOs alone and duplexes), T_m was determined as described in ref *38*. Duplex melting occurred at high temperature in a reversible fashion, which helps to distinguish this transition from triplex melting.

Electrophoretic Mobility Shift Assays (EMSA). Oligonucleotides were labeled at the 5′-end with [γ-^{32}P]ATP (Amersham) using a T4 polynucleotide kinase (Invitrogen) according to the manufacturer's protocol. Duplexes were formed by annealing the 5′-end-labeled purine-rich strand with the unlabeled complementary strand in 10% molar excess in 50 mM NaCl. Binding reactions were performed as follows: Duplex at 10 nM (40 RY) was incubated with increasing concentrations of TFOs for 72 h at 20 °C in binding buffer (2.5 mM NaCl, 140 mM KCl, 0.5 mg/mL tRNA, and 10% sucrose with either 50 mM HEPES or 50 mM MES) with or without $MgCl_2$ or with increasing concentrations of $CuCl_2$. The mixture was then loaded on a 10% native acrylamide gel in 50 mM MES, pH 6.0, or in

[1] Abbreviations: EMSA, electrophoretic mobility shift assay; TFO, triplex-forming oligonucleotide; mC, 5-methylcytosine; mo, morpholino.

Table 1: List, Sequences, and Characteristics of the Oligonucleotides Used in This Study[a]

name	sequence	backbone/sugar	base
19 R	5′-cttgccAAGAGAGcatgtc-3′		
19 Y	3′-gaacggTTCTCTCgtacag-5′		
7TC	5′-TTCTCTC-3′		
7TmC	5′-TTMTMTC-3′		mC
26 R	5′-cttgccAAGAGAGAAGAGAGcatgtc-3′		
26 Y	3′-gaacggTTCTCTCTTCTCTCgtacag-5′		
14TC	5′-TTCTCTCTTCTCTC-3′		
14TmC	5′-TTMTMTMTTMTMTC-3′		mC
33 R	5′-cttgccAAGAGAGAAGAGAGAAGAGAGcatgtc-3′		
33 Y	3′-gaacggTTCTCTCTTCTCTCTTCTCTCgtacag-5′		
21TC	5′-TTCTCTCTTCTCTCTTCTCTC-3′		
21TmC	5′-TTMTMTMTTMTMTMTTMTMTC-3′		mC
21TCOMe	5′-UUCUCUCUUCUCUCUUCUCUC-3′	OMe	U
21TCmo	5′-TTCTCTCTTCTCTCTTCTCTC-3′	PNN/mo	
40 R	5′-cttgccAAGAGAGAAGAGAGAAGAGAGAAGAGAGcatgtc-3′		
40 Y	3′-gaacggTTCTCTCTTCTCTCTTCTCTCTTCTCTCgtacag-5′		
28TC	5′-TTCTCTCTTCTCTCTTCTCTCTTCTCTC-3′		
28TmC	5′-TTMTMTMTTMTMTMTTMTMTMTTMTMTC-3′		mC

[a] Column 1 lists the abbreviated names of the oligonucleotides, column 2 lists the primary sequences of the oligonucleotides, and columns 3 and 4 list the DNA backbone, sugar, and base chemistry. The following convention is used for the abbreviated names: the length of the oligomer in nucleotides is followed by the nature of the strand involved in the Watson−Crick duplex (R or Y) or the nature of the third strand (TC, TmC, TCOMe, and TCmo). The *Drosophila* satellite target duplexes contain one to four satellite repeats [the main repeat comprises seven base pairs (AAGAGAG/CTCTCTT)] surrounded by six base pairs at both ends in order to stabilize duplex formation and prevent partial slipped duplexes. Except where otherwise stated, oligonucleotide backbones are phosphodiester, sugar is 2′-H, and bases are natural. Abbreviations: R = adenine and guanine; Y = thymine and cytosine; M = mC = 5-methyldeoxycytosine; OMe = 2′-*O*-methyl RNA; U = deoxyuracyl; PPN/mo = phosphorodiamidate morpholino.

50 mM HEPES, pH 7.2, with or without $MgCl_2$. Gels were dried for analysis. In all cases, migration of the triple helical complexes was compared with that of the duplex (40 RY) and that of the single-stranded component of the duplex (40 R). All gels were analyzed on a phosphorimager instrument (Molecular Dynamics). The apparent dissociation constant (K_D) was calculated by plotting the remaining fraction of the duplex against TFO concentrations (8−32 determinations for each set of experimental conditions) and fitting the data with a Kaleidagraph fitting function assuming a 1:1 stoichiometry, one TFO per duplex, and an unknown K_D and using a simple mass action law ($K_D = [TFO][D^*]/[T^*]$, where [D*] and [T*] represent respectively the concentration of the radiolabeled duplex and triplex species). Taking into account the fact that the TFO is in large excess as compared to the radiolabeled duplex, we can assume that the concentration of the TFO corresponds to its initial concentration C_0. The equation used for the fitting procedure is then $\%\ D^* = 100/(1 + C_0/K_D)$.

RESULTS

Targets and Oligonucleotides. A repeated sequence (*4*) of seven base pairs (5′-AAGAGAG/5′-CTCTCTT)$_n$ was used to investigate triplex formation with natural and modified pyrimidine oligonucleotides. This AG-rich repeat is a satellite sequence present in each *D. melanogaster* centromere and represents up to 1.5% of the whole genome (*4*, *39*). Target duplexes included one to four repeats of the satellite sequence surrounded by six base pairs (Table 1).

All TFOs were designed to form pyrimidine-parallel triple helices. 7TC, 14TC, 21TC, and 28TC were unmodified oligodeoxynucleotides. The 7TmC through 28TmC were 5-methyldeoxycytosine-containing oligodeoxynucleotides (*29*). The 21TCOMe was modified with 2′-*O*-methyl on its sugar (*31*) whereas in the 21TCmo the phosphodiester backbone was replaced by phosphorodiamidate and the sugar replaced by a morpholino subunit (*40*) (Table 1).

Triple Helices with Natural and Modified Oligonucleotides: UV Melting Curve Analysis. Formation of pyrimidine triple helices can be monitored by following UV absorbance. To avoid experimental artifacts, we first analyzed the behavior of the individual strands as a function of temperature. Self-association of a TFO may lead to a transition that could be inappropriately attributed to triplex formation (*41*). No transition was obtained with the TFOs alone in the absence of Mg^{2+} at pH 7.2. A very unstable structure was observed at pH 6.0 with 10 mM $MgCl_2$ for the 14TC and 21TC and a more stable structure (with a $T_m = 22$ °C) was observed with the 28TC (Figure 1A). 5-Methyl-C-containing TFOs exhibited the same behavior as the phosphodiester TFOs (data not shown). We then analyzed the behavior of the duplexes. A single transition was obtained by mixing the 19 R and 19 Y strands, 26 R and 26 Y strands, 33 R and 33 Y strands, and 40 R and 40 Y strands (data not shown; $T_m = 64$, 69, 73, and 74 °C for 19 RY, 26 RY, 33 RY, and 40 RY duplexes, respectively). When the duplexes were mixed with a TFO, two transitions were generally observed: the one occurring at high temperature corresponds to the dissociation of the duplex, while the other transition corresponds to the dissociation of the third strand (illustrated in Figure 1B).

At pH 6.0 with 5 mM $MgCl_2$ a transition due to the dissociation of the TFO from the duplex was observed with the 28TC, 21TC, and 14TC with $T_{1/2}$ values of 60, 52, and 38 °C, respectively. No transition was observed with the 7TC (see Table 2 and Figure 1B, open circles). Therefore, triple helix stability appeared to be dependent on TFO length. A similar effect was observed with the 14−28 TmC TFOs (see Table 2) except that all $T_{1/2}$ values were higher, reflecting an increase in triplex stability due to cytosine methylation. As the 28TmC triplex and the duplex transitions appeared

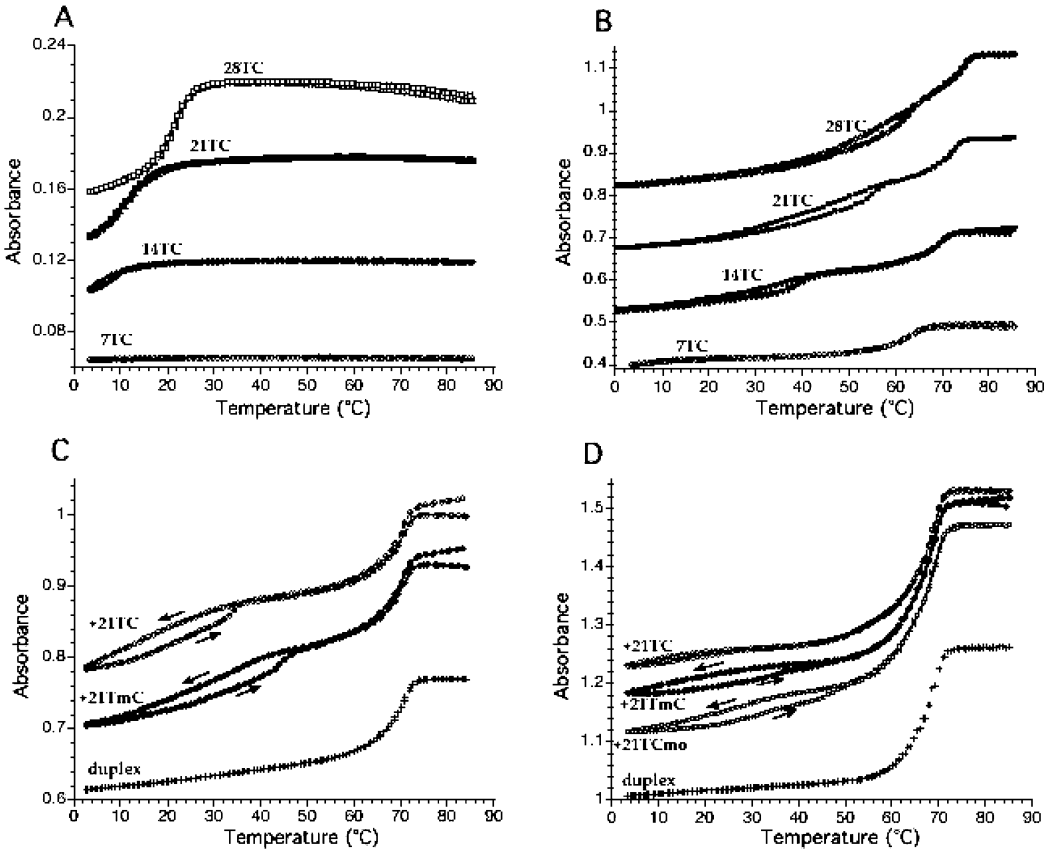

FIGURE 1: UV melting curves. (A) Self-association of the TFOs. For purposes of clarity, only the melting profiles of the unmodified TFOs (7TC, 14TC, 21TC, and 28TC) are shown. Experimental conditions: 10 mM sodium cacodylate, pH 6.0, 0.1 M KCl, 5 mM $MgCl_2$, and 2.5 μM strand concentration. (B) Triplex formation at acidic pH. Slight hysteresis is observed. Experimental conditions: 10 mM sodium cacodylate, pH 6.0, 0.1 M KCl, 5 mM $MgCl_2$, 1.5 μM duplex strand concentration, and 1.8 μM third strand. The name of the TFO is indicated for each curve. (C) Triplex formation at neutral pH. Strong hysteresis is observed. Directions of temperature changes are shown with arrows. Experimental conditions: 10 mM sodium cacodylate, pH 7.0, 0.1 M KCl, 5 mM $MgCl_2$, 1.5 μM duplex strand concentration, and 1.8 μM third strand. (D) Triplex formation in the absence of magnesium. Strong hysteresis is observed. Directions of temperature changes are shown with arrows. Experimental conditions: 10 mM sodium cacodylate, pH 7.2, 0.14 M KCl, 2.5 μM duplex strand concentration, and 3 μM third strand.

Table 2: $T_{1/2}$ Values for the Triplex-Forming Oligonucleotides Used in This Study[a]

	$T_{1/2}$ (°C)				
	pH 6.0, 100 mM KCl, 5 mM $MgCl_2$[b]	pH 6.5, 100 mM KCl, 10 mM $MgCl_2$[b]	pH 7.1, 100 mM KCl, 10 mM $MgCl_2$[b]	pH 7.0, 100 mM KCl, 5 mM $MgCl_2$[b]	pH 7.2, 140 mM KCl, no $MgCl_2$[c]
7TC	<0[d] (63)	–	–	<0[d] (63)	<0[d] (63)
14TC	38 (69)	–	–	–	<10 (69)
21TC	52 (73)	40 (73)	–	25 (73)	15 (73)
28TC	60 (74)	–	–	–	28
7TmC	nd	–	–	–	–
14TmC	48 (69)	–	–	–	–
21TmC	60 (73)	54 (73)	39 (73)	37 (73)	30 (73)
28TmC	>65[e] (74)	–	–	–	–
21TCOMe	–	54 (73)	35 (73)	–	35[f] (73)
21TCmo	–	>65[e] (73)	48 (73)	41 (73)	40 (73)

[a] In most cases, hysteresis is present; the values provided here correspond to the heating curve and lead to an overestimation of the equilibrium T_m. All values were determined at 260 or 245 nm. Numbers in parentheses indicate the T_m of the corresponding duplexes (all T_m and $T_{1/2}$ are given with an uncertainty of ±2 °C). A dash means not determined. [b] 1.5 μM duplex, 1.8 μM TFO. [c] 2.5 μM duplex, 3 μM TFO. [d] No transition. [e] Transition intermingled with duplex melting. [f] The transition is spread over a large temperature range, making an accurate determination of $T_{1/2}$ difficult.

to be intermingled, it is not possible to determine an accurate $T_{1/2}$ value (Figure S1A). Nevertheless, the amplitude of the transition observed with 28TmC + 40 RY is larger than the amplitude of the 40 RY duplex alone, in agreement with triplex formation. Further evidence that the 28TmC can form a triplex were obtained by EMSA experiments (K_D = 0.9 μM at 4 °C, pH 7.0; Figure S1B) and by melting experiments at neutral pH ($T_{1/2}$ = 30 °C; Figure S1A).

All triplexes were strongly pH-dependent. The stability of all triplexes was decreased at near-neutral pH. A variety of experimental conditions were chosen (details provided in Table 2). Increasing the pH from 6.0 to 7.0 in the presence

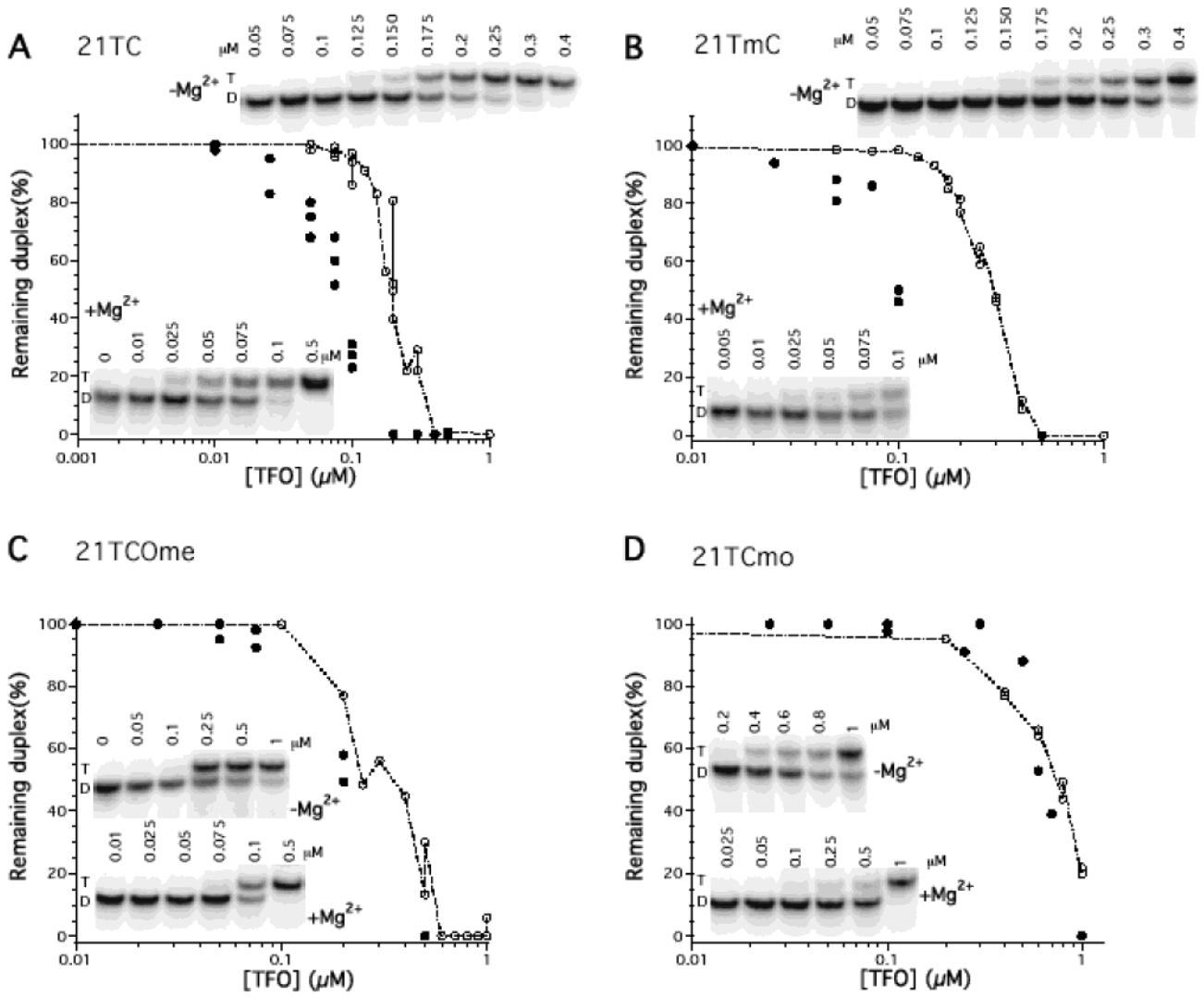

FIGURE 2: EMSA with the *Drosophila* satellite triplex-forming oligonucleotides at pH 6.0. The triplex formation was monitored by EMSA experiments. All gels were quantified using a phosphorimager. Results were analyzed by plotting the fraction of the remaining duplex band against TFO concentrations. No fit was simply applicable because of the strong cooperativity of the third strand binding. (A) 21TC with (filled circles) or without (open circles) $MgCl_2$; (B) 21TmC with (filled circles) or without (open circles) $MgCl_2$; (C) 21TCOMe with (filled circles) or without (open circles) $MgCl_2$; (D) 21TCmo with (filled circles) or without (open circles) $MgCl_2$. For each set of experiments, a representative EMSA is provided as an example. All EMSA experiments were performed as follows: Radiolabeled double-stranded target (40 RY) was incubated with increasing concentrations of TFO in the absence or presence of $MgCl_2$. 10 nM radiolabeled 40 RY was incubated with 21TC, 21TmC, 21TCOMe, or 21TCmo for 72 h in buffer containing 50 mM MES, pH 6.0, 2.5 mM NaCl, 140 mM KCl, 0.5 mg/mL tRNA, and 10% sucrose with or without 10 mM $MgCl_2$ at 20 °C. Samples were separated on a 10% nondenaturing acrylamide gel in 50 mM MES, pH 6.0 at room temperature. All TFO concentrations are given in μM. T = triplex; D = duplex.

of 5 mM $MgCl_2$ led to a concomitant decrease in $T_{1/2}$ for the 21TC and 21TmC oligonucleotides. At neutral pH, the 21TmC was still able to form a stable triplex ($T_{1/2} = 37$ °C) while the 21TC triplex was destabilized but still gave rise to a transition with a $T_{1/2}$ value of 25 °C (Table 2 and Figure 1C). In a similar fashion, in the presence of 10 mM $MgCl_2$, a modest increase in pH (from 6.5 to 7.1) led to a 15−20 °C decrease in $T_{1/2}$ for the 21TmC, 21TCOMe, and 21TCmo oligonucleotides (Table 2).

We next investigated the magnesium contribution to triplex stability. Melting experiments were performed in the absence of $MgCl_2$ in a 10 mM sodium cacodylate and 140 mM potassium chloride buffer (i.e., close to physiological monocation concentrations). The T_ms of the duplexes were marginally affected by these changes (compare crosses on Figure 1C,D). At pH 7.2 without magnesium chloride, the 21TC could not form a stable triplex ($T_{1/2} < 20$ °C) whereas the triplex formed with the 21TmC was still present. Under both conditions, 21TCmo formed a stable triplex with comparable $T_{1/2}$ values (Table 2 and Figure 1D).

These results allowed us to conclude that the *D. melanogaster* $(AAGAGAG)_n$ satellite repeat is able to accommodate a three-stranded structure, exhibiting classical pyrimidine triplex features plus a length dependency.

Triple Helices with Natural and Modified Oligonucleotides: EMSA Analysis. Formation of triple helices was confirmed by EMSA (examples provided in Figures 2−4 and in Figures S2 and S3): binding of a third strand slows down the migration of the target duplex. By varying the TFO concentration and repeating the experiment at least two to five times, it was possible to determine an apparent dissociation constant (K_D). In all experiments, we used the 40

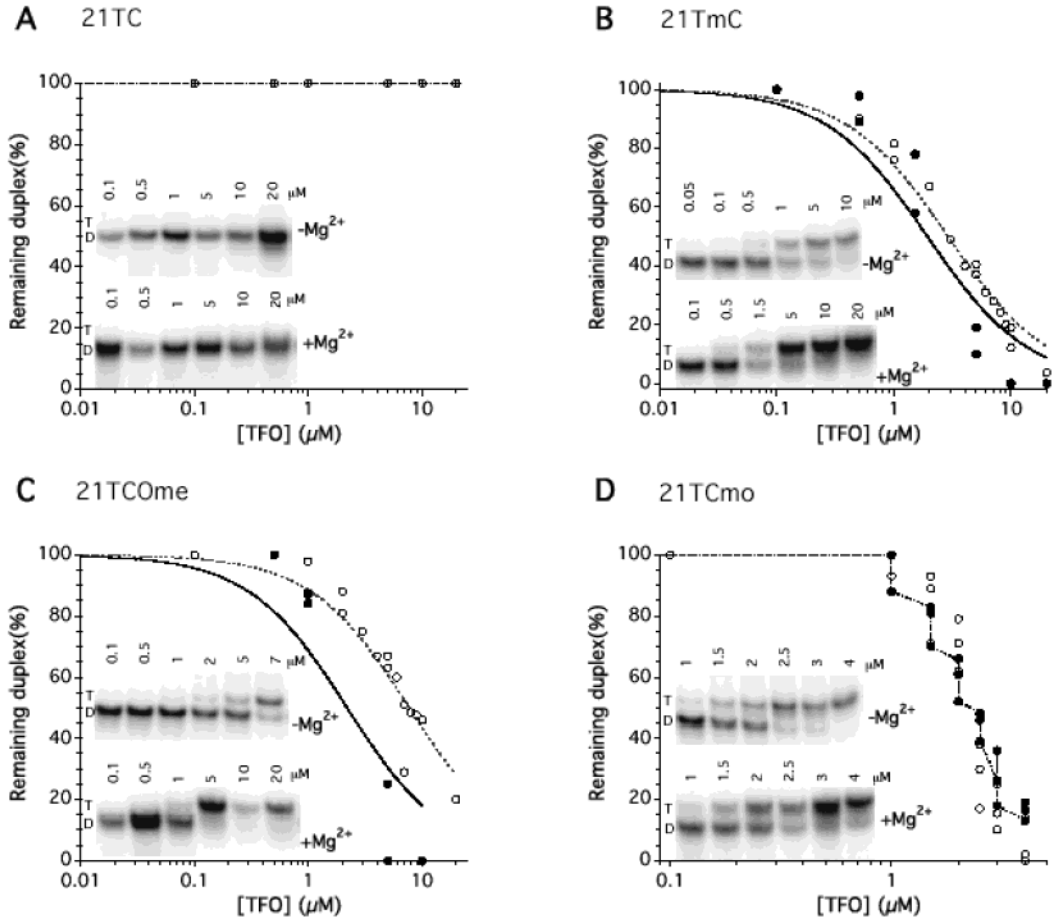

FIGURE 3: EMSA with the *Drosophila* satellite triplex-forming oligonucleotides at pH 7.2. The triplex formation was monitored by EMSA experiments. All gels were quantified using a phosphorimager. Results were analyzed by plotting the fraction of the remaining duplex band against TFO concentrations and fitting the data with a Kaleidagraph fitting function assuming a 1:1 stoichiometry, one TFO per duplex, and an unknown K_D and using a simple mass action law, taking into account the fact that the TFO is in large excess as compared to the radiolabeled duplex. (A) 21TC with (filled circles) or without (open circles) $MgCl_2$; (B) 21TmC with (filled circles) or without (open circles) $MgCl_2$; (C) 21TCOMe with (filled circles) or without (open circles) $MgCl_2$; (D) 21TCmo with (filled circles) or without (open circles) $MgCl_2$. For each set of experiments, a representative EMSA is provided as an example. All EMSA experiments were performed as follows: Radiolabeled double-stranded target (40 RY) was incubated with increasing concentrations of TFO in the absence or presence of $MgCl_2$. 10 nM radiolabeled 40 RY was incubated with 21TC, 21TmC, 21TCOMe, or 21TCmo for 72 h in buffer containing 50 mM HEPES, pH 7.2, 2.5 mM NaCl, 140 mM KCl, 0.5 mg/mL tRNA, and 10% sucrose with or without 10 mM $MgCl_2$ at 20 °C. All TFO concentrations are given in μM. T = triplex; D = duplex.

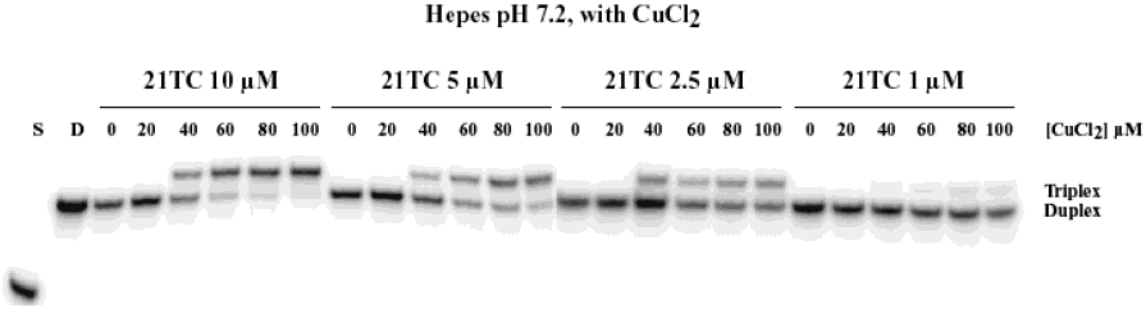

FIGURE 4: EMSA with the *Drosophila* satellite triplex-forming oligonucleotides in the presence of Cu^{2+} at pH 7.2. All incubations were performed as follows: Radiolabeled double-stranded target (40 RY) was incubated in the presence of various concentrations of 21TC (10, 5, 2.5, and 1 μM) for 72 h at 20 °C in a buffer containing 50 mM HEPES, pH 7.2, 2.5 mM NaCl, 140 mM KCl, 0.5 mg/mL tRNA, and 10% sucrose supplemented with increasing concentrations of $CuCl_2$ (from 0 to 100 μM). Samples were migrated on a 10% nondenaturing acrylamide gel with 50 mM HEPES, pH 7.0 at room temperature. S = radiolabeled purine strand (40 R) of the duplex; D = duplex 40 RY alone.

RY duplex as a target and the 21mers as third strands. This choice was made because the 28mers showed significant self-association in UV melting experiments whereas the 7mers and 14mers gave less stable triplexes (see Figure 1 or Table 2). K_D at 20 °C were determined after a 72 h incubation, ensuring complete thermodynamic equilibrium (no significant variation in binding was observed with longer incubations; data not shown).

At pH 6.0, in the presence of 140 mM KCl and 2.5 mM NaCl and in the absence of divalent cations, all TFOs were

Table 3: K_D Values (μM) for the Triplex-Forming Oligonucleotides Used in This Study[a]

	K_D (μM)					
	pH 6.0, no dication[b]	pH 6.0, 10 mM Mg^{2+} [c]	pH 7.2, no dication[d]	pH 7.2, 10 mM Mg^{2+} [e]	pH 7.2, 100 μM Cu^{2+} [f]	pH 7.2, 40 μM Cu^{2+} [g]
21TC	0.25 ± 0.05	0.07 ± 0.01	−	−	3.0 ± 0.5	12.4 ± 0.6
21TmC	0.4 ± 0.1	0.15 ± 0.03	3.3 ± 0.2	1.9 ± 0.4	1.0 ± 0.3	1.8 ± 0.4
21TCOMe	0.26 ± 0.07	0.23 ± 0.06	8.7 ± 1.2	2.2 ± 0.8	1.7 ± 0.4	4.6 ± 0.4
21TCmo[h]	0.8 ± 0.2	0.8 ± 0.2	2.2 ± 0.5	2.4 ± 0.4	0.9 ± 0.5	1.9 ± 1.1

[a] All apparent dissociation constants, K_D (μM), were calculated by fitting the percent of the remaining duplex band (duplex fraction) versus the concentration of TFO. All experiments with the 21 base pair long oligomers and the 40 RY duplex were repeated in two to five independent experiments. In each case, K_D values were calculated from 8 to 36 determinations of the fraction of the remaining duplex. Data were fitted assuming a 1:1 stoichiometry between the duplex and the TFO, in agreement with the presence of a single retarded band at the expected position. [b] Incubation was performed in 50 mM MES, pH 6.0, 2.5 mM NaCl, and 140 mM KCl for 72 h at 20 °C. [c] Incubation was performed in 50 mM MES, pH 6.0, 2.5 mM NaCl, 140 mM KCl, and 10 mM $MgCl_2$ for 72 h at 20 °C. [d] Incubation was performed in 50 mM HEPES, pH 7.2, 2.5 mM NaCl, and 140 mM KCl for 72 h at 20 °C. [e] Incubation was performed in 50 mM HEPES, pH 7.2, 2.5 mM NaCl, 140 mM KCl, and 10 mM $MgCl_2$ for 72 h at 20 °C. [f] Incubation was performed in 50 mM HEPES, pH 7.2, 2.5 mM NaCl, 140 mM KCl, and 100 μM $CuCl_2$ for 72 h at 20 °C. [g] Incubation was performed in 50 mM HEPES, pH 7.2, 2.5 mM NaCl, 140 mM KCl, and 40 μM $CuCl_2$ for 72 h at 20 °C. A dash indicates no triplex formation. [h] For this TFO, the concentration dependency of the duplex and triplex species does not obey the simple mathematical model described in Experimental Procedures (see Figures 3D and 5D for examples).

able form triplexes (Table 3 and Figure 2). K_D were comparable for the 21TC (0.25 ± 0.05 μM) and 21TCOMe (0.26 ± 0.07 μM) oligonucleotides, whereas the 21TmC showed a slightly higher K_D (0.4 ± 0.1 μM) and the morpholino oligonucleotide and 21TCmo a 3-fold higher K_D (0.8 ± 0.2 μM). Under the same conditions but in the presence of 10 mM $MgCl_2$ (Table 3 and Figure 2), the K_D were significantly improved (i.e., lowered approximately 3-fold) for the 21TC (0.07 ± 0.01 μM) and 21TmC (0.15 ± 0.03 μM) TFOs. No stabilization was noted for the 21TCOMe ($K_D = 0.23 \pm 0.06$ μM) or for the 21TCmo ($K_D = 0.8 \pm 0.2$ μM).

At pH 7.2 with no magnesium, triple helix formation was abolished for 21TC (Figure 3A). Modified TFOs were still able to form a triple helix with a K_D 3 times higher for the 21TCmo (2.2 ± 0.5 μM), 9 times higher for the 21TmC (3.3 ± 0.2 μM), and 40 times higher for the 21TCOMe (8.7 ± 1.2 μM) than those observed at pH 6.0 (Table 3 and Figure 3B−D). In the presence of 10 mM $MgCl_2$, K_D were improved from 3.3 to 1.9 μM for the 21TmC and from 8.7 to 2.2 μM for the 21TCOMe. As previously demonstrated at pH 6.0, the 21TCmo hybridization with the target duplex appeared again to be magnesium-independent ($K_D = 2.2 \pm 0.5$ and 2.4 ± 0.4 μM with or without 10 mM $MgCl_2$, respectively).

Results described here are in general agreement with what was observed with UV melting experiments and confirm that the *D. melanogaster* $(AAGAGAG)_n$ satellite repeat can form a classical pyrimidine triplex in vitro. However, one should note that, in T_m experiments, the 21TCmo oligonucleotide allowed the formation of the most stable triplex under a variety of experimental conditions (see Table 2) whereas this observation was not confirmed for all EMSA experiments (Table 3). Such differences could be the result of kinetic factors and/or illustrate the observation that a higher T_m does not necessarily reflect a higher stability ($\Delta G°$) at a given temperature, depending on the enthalpy of the reaction. Another reason we observe differences between T_m and EMSA experiments could be because they were not performed strictly under the same conditions of pH and salinity.

Triple Helices with Natural and Modified Oligonucleotides in the Presence of Cu^{2+}: EMSA Analysis. The effect of Cu^{2+} on triple helix formation was then investigated. No $CuCl_2$ concentration higher than 100 μM was tested because precipitation occasionally occurred under these conditions. This precipitation was even more pronounced for UV melting experiments and prevented a reliable analysis of the melting profile in the presence of copper. For these reasons, results concerning the effects of Cu^{2+} on triple helix formation were based solely on EMSA experiments, which are reported in Figures 4 and S3 and their quantification in Figure 5).

At pH 7.2 in 140 mM KCl and 2.5 mM NaCl, the natural phosphodiester TFO 21TC does not form a triple helix, as shown in Figures 3A, 4 (lines 0 μM $CuCl_2$), and 5A. This inability was overcome in the presence of 40 μM $CuCl_2$ or higher (Figures 4 and 5A). No triplex formation was observed below 40 μM $CuCl_2$ even for higher 21TC concentrations (data not shown). For 10 μM 21TC, 100 μM Cu^{2+} allowed 96% triplex formation, and this ability decreased proportionally with 21TC concentration: 64% of the triplex was formed at 5 μM 21TC, 39% at 2.5 μM, and only 15% at 1 μM. No triplex formation was seen with 0.5 μM 21TC. Triple helix formation with modified TFOs was also improved with increasing Cu^{2+} concentrations (see Figures 5B,C,E and S3; those TFOs were already able to form a triplex at pH 7.2, in the absence of divalent cations).

At low oligonucleotide concentration (0.5 μM 21TC, 0.1 μM 21TmC, 0.2 μM 21TCOMe, 0.5 μM 21TCmo) where none of the TFOs can form a triple helix at pH 7.2, the addition of $CuCl_2$ was unable to promote triplex formation. These observations suggest that Cu^{2+} could shift the reaction equilibrium toward triplex formation by changing the local binding conditions but that the binding limit was still dictated by the TFO concentration. Furthermore, the capacity of $CuCl_2$ to overcome pH dependency and to allow binding of the 21TC at pH 7.2 is only partial, as the resulting K_D are still higher than at pH 6.0 (see Table 3).

To compare the effect of Cu^{2+} on triple helix formation, K_D were determined by plotting the fraction of the remaining duplex versus the TFO concentration for a given concentration of $CuCl_2$. For each oligonucleotide, K_D variations were plotted versus the $CuCl_2$ concentrations (Figure 5E). The presence of Cu^{2+} promoted the binding of the 21TC TFO to the 40 RY duplex, and the related K_D ranged from 12.4 μM (for 40 μM Cu^{2+}) to 3.0 μM (for 100 μM Cu^{2+}). No binding was observed for $Cu^{2+} \leq 20$ μM. The K_D of the modified TFOs were lowered (for $CuCl_2$ concentrations ranging from

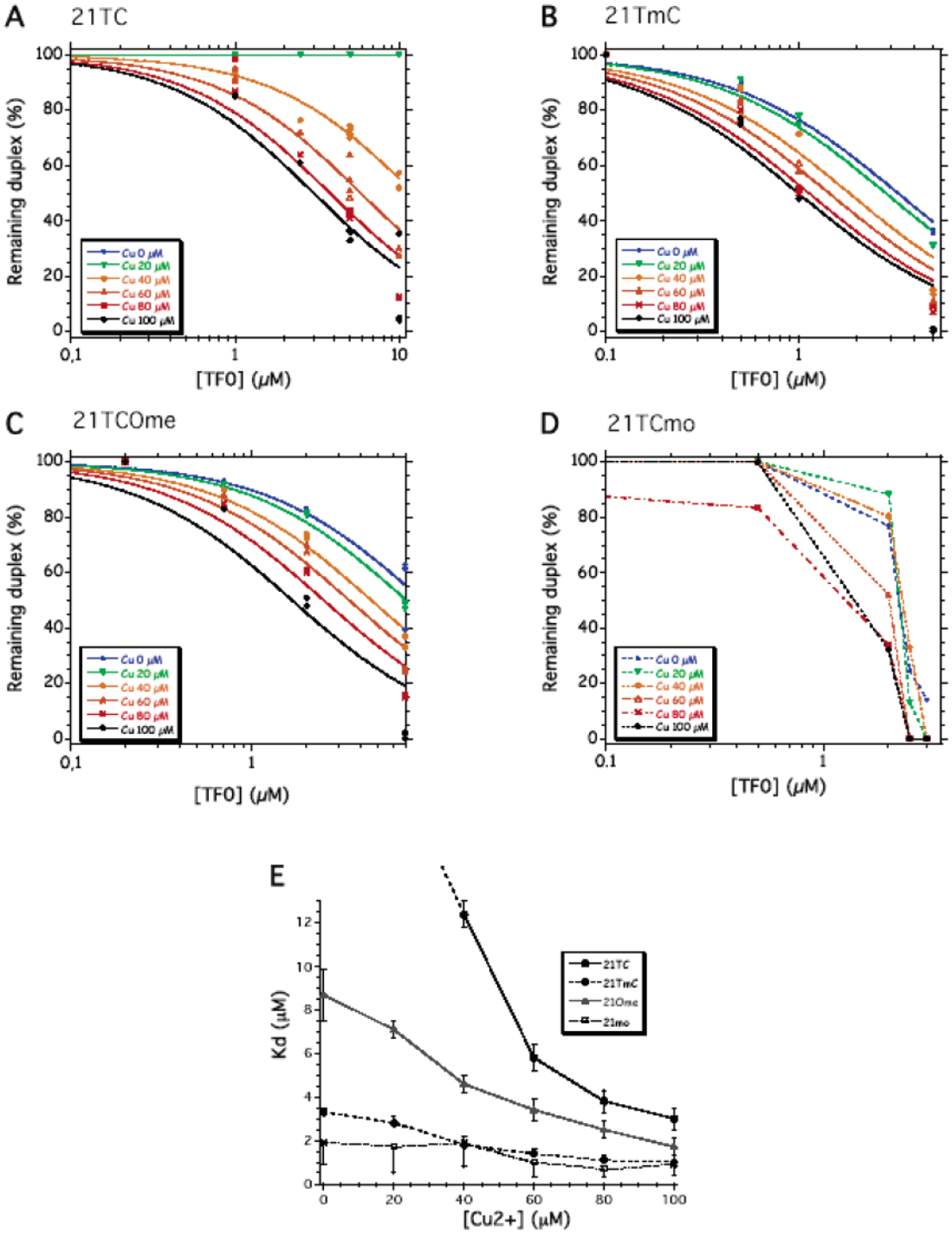

FIGURE 5: Copper concentration dependency of the triplex formation for different TFOs. (A−C) K_D were calculated by plotting and fitting the fraction of remaining duplex determined from EMSA experiments versus TFO concentration for a given concentration of $CuCl_2$. Examples of EMSA are given in Supporting Information. (A) Fit for the 21TC oligonucleotide. 21TC concentrations range from 0 to 10 μM. $CuCl_2$ concentrations range from 0 to 100 μM. (B) Fit for the 21TmC oligonucleotide. 21TmC concentrations range from 0 to 5 μM. $CuCl_2$ concentrations range from 0 to 100 μM. (C) Fit for the 21TCOMe oligonucleotide. 21TCOMe concentrations range from 0 to 7 μM. $CuCl_2$ concentrations range from 0 to 100 μM. (D) Binding of the 21TCmo oligonucleotide. 21TCmo concentrations range from 0 to 3 μM. $CuCl_2$ concentrations range from 0 to 100 μM. No fit was applied here because the triplex formation is not following a simple mass action law. (E) For each TFO, the K_D was plotted against the corresponding $CuCl_2$ concentration: filled circles, 21TC; filled diamonds, 21TmC; filled triangles, 21TCOMe; open squares, 21TCmo. For purposes of clarity, only the upper and lower parts of error bars are presented for 21TmC and 21TCmo, respectively.

0 to 100 μM) from 3.3 ± 0.2 to 1.0 ± 0.3 μM for 21TmC and from 8.7 ± 1.2 to 1.7 ± 0.4 μM for 21TCOMe (Table 3 and Figure 5). Cu^{2+} was not able to stabilize clearly the 21TCmo triplex (see Figure 5D,E).

At pH 7.2, the stabilizing effects of $CuCl_2$ and $MgCl_2$ appeared to be quite different. First, stabilization of the triple helix by Cu^{2+} was much more efficient than stabilization by Mg^{2+}. A 100-fold lower copper concentration (100 μM $CuCl_2$ versus 10 mM $MgCl_2$) led to an equal or lower K_D as compared to $MgCl_2$ (Table 3). Second, the stabilization depended on the chemical modification of the TFO. For Cu^{2+} it applied to all TFOs except for the morpholino one and

could be ordered as follows: 21TC > 21TmC > 21TCOMe > 21TCmo = 0, while for Mg^{2+} it only applied to the 21TCOMe and 21TmC oligonucleotides.

DISCUSSION

Triple Helix Formation. We have shown in this study that a *D. melanogaster* AG-rich satellite DNA $(AAGAGAG)_n$, present in the centromeric heterochromatin of all chromosomes, may form a parallel pyrimidine triplex in vitro. As revealed by UV spectroscopic studies and EMSA experiments, this pyrimidine triple helix exhibited classical features such as pH dependency and stabilization by Mg^{2+} counterions. The use of base-modified TFOs such as 5-methyl-dC and backbone-modified TFOs such as 2′-*O*-methyl led to the stabilization and reduced pH dependency of triplex formation. Whichever TFO was used, the most stable triplexes were obtained with long TFOs (21mers and 28mers). This length dependency, although not unexpected, has never been reported in the context of a short (seven base) repetitive motif. To our knowledge, this is the first report of triplex formation on a target with a variable number (1−4) of specific oligopurine−oligopyrimidine motifs. The significant difference in $T_{1/2}$ between three and four repeats suggests that this stability could be further increased with longer sequences (five repeats or more). However, two problems should be noted with long oligonucleotides. First, self-association phenomena are more pronounced for longer TFOs (see Figure 1A). Second, melting of the triplex appears to be complex, with a biphasic character (see Figure 1B). At this time, we cannot predict the practical limit of the number of TTCTCTC repeats that can be incorporated in a TFO (dozens/hundreds of consecutive AAGAGAG/CTCTCTT tracts may be found in the *Drosophila* genome).

The Morpholino Case. The triplex formation with the morpholino oligonucleotide, at pH 7.2 without magnesium chloride, gave a K_D consistent with the results obtained with other morpholino TFOs (L. Lacroix et al., in preparation; *34*). Surprisingly, the 21TCmo appeared to be the least sensitive to increasing pH from 6.0 to 7.2, as its K_D is only lowered 3-fold (versus 15- and 40-fold for 21TmC and 21TCOMe, respectively) in the absence of $MgCl_2$. This result confirms what Lacroix et al. have already observed with a 16mer morpholino TFO (*34*) but is in contradiction with what Basye et al. observed in the Her-2/neu promoter as their morpholino TFOs exhibit poor binding at pH 7.2 (*35*). Little is known about triplex formation with morpholino TFOs, but it is now clear that the behavior of such TFOs is not canonical. This is in line with the observation that, for all EMSA experiments with 21TCmo, the concentration dependency of the remaining duplex band cannot be properly fitted with a simple model. In addition, the effect of magnesium ions is completely different for the 21TCmo compared to the other TFOs used in this study and to DNA TFOs in general. Magnesium ions are known to stabilize and accelerate the formation of pyrimidine DNA triplexes (*38*, *42*−*44*). In contrast, we found that the triplex formation with 21TCmo was independent of the presence of Mg^{2+} and Cu^{2+} ions, and Lacroix et al. have even shown that $MgCl_2$ hinders morpholino triple helix formation (*34*). As Mg^{2+} ions principally interact with the negative phosphate charges (*45*), one may propose that this behavior is the result of the uncharged morpholino backbone.

Cu^{2+} versus Mg^{2+}. As already elucidated, magnesium strongly favors purine intermolecular triplex formation and can improve stability of both purine and pyrimidine triplexes (*38*, *42*−*44*, *46*). In our experiments, we showed that magnesium ions did favor pyrimidine triple helix formation (both at pH 6.0 and at pH 7.2) but were not an absolute requisite, in contrast to the case of purine triplexes (*15*, *19*).

When copper(II) chloride was added to the hybridization reaction, we observed a rather different effect on triple helix formation. Cu^{2+} appeared to stabilize the triple helix in a more efficient manner than Mg^{2+}, as the required copper concentrations were 10−100 times lower. The Cu^{2+} stabilizing effect was very pronounced for the 21TC and 21TCOMe oligonucleotides (see Figure 5). Cu^{2+} also significantly stabilized the 21TmC triplex but to a lesser extent (Figure 5, diamonds; $K_D = 3.3 \pm 0.2\ \mu M$ in the absence of Cu^{2+} and $1.0 \pm 0.3\ \mu M$ with 100 μM Cu^{2+}). In contrast, the small decrease in K_D obtained with 21TCmo was not statistically significant (Figure 5, squares): the morpholino oligonucleotide is as insensitive to the presence of Cu^{2+} as it is to the presence of Mg^{2+}.

The main difference between Cu^{2+} and Mg^{2+}, however, was the capacity of the former to allow formation of a triple helix, at physiological pH, with the 21TC. This is, to our knowledge, the first in vitro demonstration that a modification of the DNA environment, other than lowering pH to below 7.0 and adding spermine or organic cosolvent (*22*), can promote the formation of a pyrimidine triplex with an unmodified phosphodiester TFO. This effect is clearly not a peculiar feature of the *Drosophila* satellite sequence as we have observed the same effect for other polypurine−polypyrimidine sequences (Lacroix et al., in preparation). This observation suggests that copper may be an important factor for pyrimidine triplex formation and stabilization at pH 7.0 in vitro. However, we cannot presently assess if copper is a general requisite for pyrimidine triplex formation at pH 7.0 as many factors, including a longer DNA chain, other divalent cations, or spermine, may permit it.

Little is known about interactions between divalent cations and pyrimidine DNA triplexes. Since Mg^{2+} association is essentially limited to nonspecific electrostatic (labile) interaction with the anionic oxygen atoms of the phosphodiester backbone (*45*), it can be assumed that its activity as a counterion is responsible for the triplex stabilization. Obviously, such an interaction with DNA cannot overcome the pH dependency of the pyrimidine triplex formation. Other divalent metal cations and especially copper ions are known to bind to DNA by forming relatively stable bond(s) with specific groups on the nucleoside (*45*). In such a context, copper ions have a preferential affinity for guanine (especially by coordination with N_7 and N_3, which are accessible in double-stranded DNA) and to a lesser extent for cytosine (by coordination with N_3 and O_2) (*45*, *47*). At the macromolecular level, Cu^{2+} has two types of binding sites as determined by flame atomic absorption spectrophotometry (*48*) and by electron paramagnetic resonance (EPR) (J. Lacoste, unpublished results), one of which results from an interaction with the bases and the other with the phosphate moiety. We envision that a Cu^{2+} ion could coordinate the N_7 of a guanine in a duplex and the N_3 and/or O_2 of atoms of cytosine in the third strand. This would allow a stabilization of the triplex without protonation of the cytosine N_3

and, as observed here, a lower pH dependence. Another possibility is that Cu^{2+} could bind without intercalation between bases by coordinating the exocyclic O_2 site of the third strand and the phosphate of the purine strand of the duplex. This would also allow a stabilization of the triplex with little structural modification. These two models are not mutually exclusive.

Biological Relevance of Triplexes in Heterochromatin. In this study, we showed that the *Drosophila* AG-rich satellite is able to form a pyrimidine triple helix in vitro. Then we demonstrated that the pH dependence of this specific triple helix formation can be overcome by relatively low Cu^{2+} concentrations. Recent studies have shown that TFOs can be hybridized in situ to nondenatured metaphase spreads and interphase nuclei (*49*) and that triplex-forming DNAs in the human interphase nucleus can be visualized with DNA probes and anti-triplex antibodies (*50*). We are now focusing our work on the possibility that this centromeric *Drosophila* region can form triple helices in vivo as the oligonucleotides we tested are good candidates for probing the heterochromatin state during the cell cycle or during stress (heat shock, chemical shock).

ACKNOWLEDGMENT

We thank L. T. Finwit for helpful discussions. Huge thanks and numerous beers are due to Dave Pearton for proofreading. We also thank Marc Block and Cécile Lelong for reading the manuscript and EA and EG for helpful discussion.

SUPPORTING INFORMATION AVAILABLE

Three figures showing 28TmC triplex formation, an example of gel quantification, and EMSA with the *Drosophila* satellite triplex-forming oligonucleotides. This material is available free of charge via the Internet at http://pubs.acs.org.

REFERENCES

1. Heitz, E. (1928) *Jahrb. Wiss. Bot. 69*, 762−818.
2. Hennig, W. (1999) *Chromosoma 108*, 1−9.
3. Henikoff, S. (2000) *Biochim. Biophys. Acta 1470*, O1−O8.
4. Verma, R. S. (1988) *Heterochromatin. Molecular and structural aspects*, Cambridge University Press, Cambridge.
5. Hoskins, R. A., Smith, C. D., Carlson, J. W., Carvalho, A. B., Halpern, A., Kaminker, J. S., Kennedy, C., Mungall, C. J., Sullivan, B. A., Sutton, G. G., Yasuhara, J. C., Wakimoto, B. T., Myers, E. W., Celniker, S. E., Rubin, G. M., and Karpen, G. H. (2002) *Genome Biol. 3*, 0085.1−0085.16.
6. Sun, X., Le, H. D., Wahlstrom, J. M., and Karpen, G. H. (2003) *Genome Res. 13*, 182−194.
7. Sun, X., Wahlstrom, J., and Karpen, G. (1997) *Cell 91*, 1007−1019.
8. Horvath, J. E., Schwartz, S., and Eichler, E. E. (2000) *Genome Res. 10*, 839−852.
9. Dillon, N., and Festenstein, R. (2002) *Trends Genet. 18*, 252−258.
10. Sunkel, C. E., and Coelho, P. A. (1995) *Curr. Opin. Genet. Dev. 5*, 756−767.
11. Zinkowski, R. P., Meyne, J., and Brinkley, B. R. (1991) *J. Cell Biol. 113*, 1091−1110.
12. Raff, J. W., Kellum, R., and Alberts, B. (1994) *EMBO J. 13*, 5977−5983.
13. Cobb, B. S., Morales-Alcelay, S., Kleiger, G., Brown, K. E., Fisher, A. G., and Smale, S. T. (2000) *Genes Dev. 14*, 2146−2160.
14. Yamada, T., Fukuda, R., Himeno, M., and Sugimoto, K. (1999) *J. Biochem. (Tokyo) 125*, 832−837.
15. Frank-Kamenetskii, M. D., and Mirkin, S. M. (1995) *Annu. Rev. Biochem. 64*, 65−95.
16. Platero, J. S., Csink, A. K., Quintanilla, A., and Henikoff, S. (1998) *J. Cell Biol. 140*, 1297−1306.
17. Jimenez-Garcia, E., Vaquero, A., Espinas, M. L., Soliva, R., Orozco, M., Bernues, J., and Azorin, F. (1998) *J. Biol. Chem. 273*, 24640−24648.
18. Mahmoudi, T., Katsani, K. R., and Verrijzer, C. P. (2002) *EMBO J. 21*, 1775−1781.
19. Malkov, V. A., Voloshin, O. N., Soyfer, V. N., and Frank-Kamenetskii, M. D. (1993) *Nucleic Acids Res. 21*, 585−591.
20. Bernues, J., Beltran, R., Casasnovas, J. M., and Azorin, F. (1990) *Nucleic Acids Res. 18*, 4067−4073.
21. Mills, M., Arimondo, P. B., Lacroix, L., Garestier, T., Hélène, C., Klump, H., and Mergny, J. L. (1999) *J. Mol. Biol. 291*, 1035−1054.
22. Moser, H. E., and Dervan, P. B. (1987) *Science 238*, 645−650.
23. Le Doan, T., Perrouault, L., Praseuth, D., Habhoub, N., Decout, J. L., Thuong, N. T., Lhomme, J., and Hélène, C. (1987) *Nucleic Acids Res. 15*, 7749−7760.
24. Beal, P. A., and Dervan, P. B. (1991) *Science 251*, 1360−1363.
25. Dittrich, K., Gu, J., Tinder, R., Hogan, M., and Gao, X. (1994) *Biochemistry 33*, 4111−4120.
26. Howard, F. B., Miles, H. T., and Ross, P. D. (1995) *Biochemistry 34*, 7135−7144.
27. Mills, M., Lacroix, L., Arimondo, P. B., Leroy, J. L., Francois, J. C., Klump, H., and Mergny, J. L. (2002) *Curr. Med. Chem.: Anti-Cancer Agents 2*, 627−644.
28. Chan, P. P., and Glazer, P. M. (1997) *J. Mol. Med. 75*, 267−282.
29. Lee, J. S., Woodsworth, M. L., Latimer, L. J., and Morgan, A. R. (1984) *Nucleic Acids Res. 12*, 6603−6614.
30. Froehler, B. C., Wadwani, S., Terhorst, T. J., and Gerrard, S. R. (1992) *Tetrahedron Lett. 33*, 5307−5310.
31. Shimizu, M., Konishi, A., Shimada, Y., Inoue, H., and Ohtsuka, E. (1992) *FEBS Lett. 302*, 155−158.
32. Escudé, C., Sun, J. S., Rougée, M., Garestier, T., and Hélène, C. (1992) *C. R. Acad. Sci., Ser. III 315*, 521−525.
33. Francois, J. C., Lacoste, J., Lacroix, L., and Mergny, J. L. (2000) *Methods Enzymol. 313*, 74−95.
34. Lacroix, L., Arimondo, P. B., Takasugi, M., Hélène, C., and Mergny, J. L. (2000) *Biochem. Biophys. Res. Commun. 270*, 363−369.
35. Basye, J., Trent, J. O., Gao, D., and Ebbinghaus, S. W. (2001) *Nucleic Acids Res. 29*, 4873−4880.
36. Cantor, C. R., Warshaw, M. M., and Shapiro, H. (1970) *Biopolymers 9*, 1059−1077.
37. Mergny, J. L., Lacroix, L., Han, X., Leroy, J. L., and Hélène, C. (1995) *J. Am. Chem. Soc. 117*, 8887−8898.
38. Rougée, M., Faucon, B., Mergny, J. L., Barcelo, F., Giovannangeli, C., Garestier, T., and Hélène, C. (1992) *Biochemistry 31*, 9269−9278.
39. Csink, A. K., and Henikoff, S. (1998) *Trends Genet. 14*, 200−204.
40. Summerton, J., Stein, D., Huang, S. B., Matthews, P., Weller, D., and Partridge, M. (1997) *Antisense Nucleic Acid Drug Dev. 7*, 63−70.
41. Lacroix, L., Mergny, J. L., Leroy, J. L., and Hélène, C. (1996) *Biochemistry 35*, 8715−8722.
42. Maher, L. J., Dervan, P. B., and Wold, B. J. (1990) *Biochemistry 29*, 8820−8826.
43. Singleton, S. F., and Dervan, P. B. (1993) *Biochemistry 32*, 13171−13179.
44. Lacroix, L., and Mergny, J. L. (2000) *Arch. Biochem. Biophys. 381*, 153−163.
45. Saenger, W. (1984) *Principles of Nucleic Acids Structure*, Springer-Verlag, New York.
46. Svinarchuk, F., Bertrand, J. R., and Malvy, C. (1994) *Nucleic Acids Res. 22*, 3742−3747.
47. Sigel, A., and Sigel, H. (1996) *Metal ions in biological systems*, Vol. 32, Marcel Dekker, New York.
48. Sagripanti, J. L., Goering, P. L., and Lamanna, A. (1991) *Toxicol. Appl. Pharmacol. 110*, 477−485.
49. Johnson, M. D., III, and Fresco, J. R. (1999) *Chromosoma 108*, 181−189.
50. Ohno, M., Fukagawa, T., Lee, J. S., and Ikemura, T. (2002) *Chromosoma 111*, 201−213.

BI049287T